Published in final edited form as:
Nat Immunol. ; 12(10): 984–991. doi:10.1038/ni.2097.

Human cytomegalovirus microRNA miR-US4-1 inhibits CD8+ T cell response by targeting the aminopeptidase ERAP1

Sungchul Kim[1], **Sanghyun Lee**[1], **Jinwook Shin**[2], **Youngkyun Kim**[1], **Irini Evnouchidou**[3], **Donghyun Kim**[1], **Young-Kook Kim**[4], **Young-Eui Kim**[5], **Jin-Hyun Ahn**[5], **Stanley R. Riddell**[6], **Efstratios Stratikos**[3], **V. Narry Kim**[4], and **Kwangseog Ahn**[1,*]

[1]National Creative Research Initiative Center for Antigen Presentation, Department of Biological Sciences, Seoul National University, Seoul 151-747, Republic of Korea

[2]Department of Molecular Genetics and Microbiology, Duke University Medical Center, Durham, NC 27710, USA

[3]Institute of Radioisotopes and Radiodiagnostic Products, National Centre for Scientific Research Demokritos, Athens, 15310, Greece

[4]Department of Biological Sciences, Seoul National University, Seoul 151-747, Republic of Korea

[5]Department of Molecular Cell Biology, Samsung Biomedical Research Institute, Sungkyunkwan University School of Medicine, Suwon, 440-746, Seoul, Republic of Korea

[6]Clinical Research Division, Fred Hutchinson Cancer Research Center, Seattle, WA 98109, USA

Abstract

The major histocompatibility complex (MHC) class I molecules present peptides on the cell surface by $CD8^+$ T cells, which is critical for killing of virally infected or transformed cells. Precursors of MHC class I-presented peptides are trimmed to mature epitopes by endoplasmic reticulum aminopeptidase 1 (ERAP1). The US2-US11 genomic region of human cytomegalovirus (HCMV) is dispensable for viral replication and harbors 3 microRNAs (miRNAs). We show here the HCMV miR-US4-1 specifically down-regulates ERAP1 expression during viral infection. Accordingly, the trimming of HCMV-derived peptides is inhibited, leading to reduced susceptibility of infected cells to HCMV-specific cytotoxic T lymphocytes (CTLs). Our findings reveal a novel viral miRNA-based CTL evasion mechanism that targets a key step in the MHC class I antigen-processing pathway.

MHC class I molecule binds peptides and presents them on the cell surface for recognition by $CD8^+$ T cells. Cytosolic peptides generated by the proteasomes and prematurely translated peptides are transported to the endoplasmic reticulum (ER) through the transporter associated with antigen processing (TAP) complex[1, 2]. Some of these peptides are further processed by ER-resident aminopeptidases, such as ERAP1, and peptide trimming by ERAP1 (also known as A-LAP, ARTS-1, and PILS-AP) in the ER is a crucial step for determining the quality and quantity of optimal antigenic peptide production and the stability of the MHC class I-β_2m-peptide heterotrimer[3–6]. ERAP1 trims relatively long

*To whom correspondence should be addressed: Department of Biological Sciences, Seoul National University, Seoul 151-747, Korea, (Phone) +822-880-9233 (Fax) +822-872-1993 ksahn@snu.ac.kr.

Authors contribution

S.K, D.K, Y-K.K and V.N.K designed and performed biochemical and cell biological experiments. J.S and Y.K performed microarray experiments. S.L, Y-E.K and J-H.A carried out the HCMV mutant generation. I.E and E.S performed *in vitro* ERAP1 trimming assay. S.R.R cloned the HCMV-specific CTLs. S.K and K.A designed the overall study and wrote the paper.

peptides efficiently in a sequence-specific manner, resulting in the accumulation of 8–9 amino acid-long optimal peptides[5, 7, 8]. ERAP1 therefore acts as a 'molecular ruler' for antigenic peptide production[9]. In addition, genome-wide association studies have associated nonsynonymous single nucleotide polymorphisms in ERAP1 with ankylosing spondylitis[4]. Additionally, ERAP1 has non-peptide processing functions via its role in shedding of cytokine receptors[4].

MiRNAs are small RNAs 19 to 23 nucleotides long that regulate gene expression by complete or partial base-pairing with the 3′-untranslated region (UTR) of their target mRNA which leads to mRNA cleavage, destabilization, or translational repression[10]. Since the first report in 2004 that viruses express miRNAs[11], numerous viral miRNAs have been discovered and are mainly related to viral proliferation and survival-related immune evasion, although this is based on a limited number of studies[12]. The β-herpesvirus HCMV expresses at least 14 miRNAs during productive infection[13, 14]. One HCMV-encoded miRNA, miR-UL112-1 targets 3 HCMV genes involved in viral replication[15], and another HCMV-encoded miRNA, miR-US25-1 can downregulate multiple host genes associated with cell cycle control and tumor progression, through interacting with the 5′-UTR of their target mRNAs[16]. In addition, miR-UL112-1 targets 1 cellular gene, MHC class I-related chain B (MICB), to escape from the natural killer (NK) cell-mediated immune response[17] and miR-UL112-1 can also repress the expression of UL114, which is antisense to the miR-UL112-1 and encodes a uracil DNA glycosylase that can influence viral replication[18]. However, the cellular or host targets of many viral miRNAs remains to be elucidated.

Many viruses have evolved strategies that target crucial stages of the MHC class I antigen presentation pathway, preventing viral peptides from being presented to $CD8^+$ T cells[1]. The 9-kb US2-US11 region within HCMV genome encodes at least 5 glycoproteins (US2, US3, US6, US10, and US11) which are specifically dedicated to interfering with the presentation of antigenic peptides to $CD8^+$ T cells[1, 19–23]. Because deletion of the US2-US11 genomic segment has no influence on viral replication[24], the US2-US11 region is considered as a reservoir of viral genes whose functions are to escape from viral antigen presentation by the MHC class I molecule.

In this study, we demonstrated that HCMV miR-US4-1 specifically targets ERAP1 and thereby inhibits the trimming of precursors to the MHC class I-presented mature epitopes, resulting in inhibition of CTL immune responses. These findings expand our understanding of the strategy of the host-virus arms race, and reinforce the notion that the US2-US11 region within HCMV genome has evolved to a reservoir of viral immunoevasins against the host $CD8^+$ T cell immune elimination of HCMV-infected cells.

Online Methods

Cell lines

U373MG cells, HEK293T cells, HFF, and HFF-TEL cells were obtained from the American Type Culture Collection (ATCC). U373MG cells, HEK293T cells, HeLa-K^b cells, HFF, and HFF-TEL cells were cultured in Dulbecco's modified Eagle's medium (Gibco) supplemented with 10% fetal bovine serum (FBS), 2 mM L-glutamine, and 50 U/ml penicillin. Dermal fibroblast cells were generated from skin biopsies and propagated in Waymouth's media (Gibco) with 15% FBS, 2 mM L-glutamine, and 50 U/ml penicillin. B3Z 86/90.14 (B3Z) hybridoma T cells were cultured in RPMI 1640 medium (Gibco) supplemented with 2 mM L-glutamine, 1 mM pyruvate, 50 mM β-mercaptoethanol, 100 U/ml penicillin, 100 mg/ml streptomycin, 10% FBS at 37°C in the presence of 5% CO_2. CTLs were cultured in HEPES-buffered RPMI supplemented with 10% human AB serum, 4 mM L-glutamine, penicillin, and streptomycin.

Viral mutagenesis

Approximately 300 bp of the miR-US4 flanking region was cloned into the pcDNA3.1 vector (Invitrogen). Six nucleotides in the hairpin of miR-US4 were mutated using site-directed PCR with the primers listed in Supplementary Table 1. Mutagenesis of bacterial artificial chromosome (BAC) of the HCMV AD169 strain was performed according to BAC modification kit (Gene Bridges). A kanamycin-selective cassette containing the US4 homologous arm was amplified using PCR with the primers listed in Supplementary Table 1. The ~200-ng mutant miR-US4 PCR products were electro-transfected into *Escherichia coli* (containing pAD/Cre) for recombination. We generated a revertant from the miR-US4 mutant BAC according to the method described above. We confirmed the mutagenesis using BAC DNA sequencing.

T cell cloning

CD8+ T cell clones specific for HCMV were prepared from peripheral blood mononuclear cells (PBMCs) of donors as previously described as described[44].

Chromium release assay

CTL clones were assayed for cytotoxic activity in a chromium release assay (CRA) using ^{51}Cr-labeled fibroblasts as target cells for HCMV RV798 infection over the indicated times. Target cells were plated in triplicate at 1.0×10^4 cells/well in 96-well round-bottom plates, and effector cells were added at various effector-to-target (E/T) ratios. After 6 h of incubation, the supernatant was harvested for γ-irradiation counting.

B3Z assay

The B3Z assay was performed as described in previous studies[36]. The LacZ activity in B3Z cells was determined by using a BetaRed β-galactosidase assay kit (EMD Biosciences, San Diego, CA) according to the manufacturer's instructions.

In vitro ERAP1 trimming assay

Human recombinant ERAP1 was expressed through infection of insect cells with baculovirus, as previously described[45]. Active ERAP1 (C-terminal 6 His tag) was harvested and purified by affinity chromatography (Ni-NTA column). Protein purity was confirmed by SDS-PAGE and activity by an established fluorigenic assay[46]. Enzymatic assays were performed as previously described[42]. For rate calculations, the total surface area of the epitope peak was measured and calibrated versus the control peptides, in order to calculate the amount of epitope produced.

Constructs

The pSuperRetro vector for siRNA or miRNA expression was purchased from OligoEngine. siRNA-GFP (control miRNA), miR-US4, miR-US4(M), miR-US5-1, siRNA-ERAP1, siRNA-ERAP1a, and siRNA-ERAP1b were constructed according to the manufacturer's instructions, using the primers shown in Supplementary Table 1. For the luciferase assay, we amplified the ERAP1a and ERAP1b 3′-UTR using the primers in Supplementary Table 1, and inserted the amplified products downstream of the luciferase gene in the pGL3-CMV vector, a modified form of the pGL3-basic vector (Promega). The 3′-UTRs of ERAP1a and ERAP1b were mutated using site-directed mutagenesis with *Pfu* DNA Polymerase (Stratagene). The pUG1 Mock, pUG1-OVA8, and pUG1-N5OVA8 vectors were previously described[34].

Antibodies

The mAb W6/32 recognizes the MHC class I HC and β_2m complex. The anti-GAPDH, anti-ERp57, and anti-Tapasin antibodies were purchased from AbFrontier (Seoul, Korea). Fluorescein isothiocyanate (FITC)-conjugated goat anti-mouse immunoglobulin G (IgG) was purchased from Jackson ImmunoResearch Laboratories. The polyclonal antibody for ERAP1 was generated by cloning a truncated cDNA encoding the C-terminal amino acids 693–941 of ERAP1b into the pET28a vector using the primers represented in Supplementary Table 1 and expressing the cloned DNA in *E. coli*. The recombinant protein was affinity-purified and used to raise rabbit anti-ERAP1 antibodies.

Microarray

RNA was assayed for quality control using Bioanalyzer 2100 (Agilent), labeled using the Low RNA Input Linear Amp Kit Plus (Agilent), and co-hybridized with labeled Universal Reference RNA (Stratagene) to an Agilent Human Whole genome 44K 4Plex. Arrays were scanned on GenePix 4000B (Axon), extracted with Agilent Feature Extraction Software, and analyzed using Genespring GX.

qRT-PCR

Total RNA was harvested using Trizol (Invitrogen). Reverse transcription was performed with M-MLV reverse transcriptase (Invitrogen) according to the manufacturer's protocol. Amplification and detection were performed with SYBR® Premix Ex Taq™ (Perfect Real Time) (TaKaRa Bio, Inc.) according to the manufacturer's protocol.

Luciferase assay

HEK293T cells were seeded in 6-well plates 1 day before transfection. For co-transfections, 10 ng firefly luciferase and 5 ng Renilla luciferase reporter plasmids were transiently transfected into cells with 2 μg pSUPER vectors. After 24–48 h, we measured luciferase activity using the dual-luciferase assay kit (Promega). Firefly luciferase activity was normalized to Renilla luciferase activity.

Flow cytometry

The expression of cell surface MHC class I was determined using a FACScalibur flow cytometer (Becton Dickinson Biosciences). Cells were harvested, washed twice with cold PBS containing 1% BSA, and incubated for 1 h at 4°C with a saturating concentration of antibodies. The cells were then washed twice with cold PBS containing 1% BSA and stained with FITC-conjugated goat anti-mouse IgG for 30 min at 4°C. A total of 10,000 gated events were collected and analyzed with CellQuest software (Becton Dickinson Biosciences).

Immunoblotting, RNA blotting, and RNase protection assay

Cells were lysed with 1% NP-40 in PBS with a protease inhibitor cocktail for 1 h at 4°C, separated by SDS-PAGE, transferred onto a nitrocellulose membrane, blocked and probed with the appropriate antibodies overnight. The membrane was washed and incubated with HRP-conjugated secondary antibody for 1 h. The immunoblots were visualized using ECL detection reagent (Pierce). RNA blotting was performed according to the previous study[47]. RPA was performed according to the manufacturer's recommendations (mirVana™ miRNA Detection Kit, Ambion).

Results

Identification of ERAP1 as a host target of miR-US4-1

Three miRNAs (miR-US4-1, miR-US5-1, and miR-US5-2) among the total 14 HCMV miRNAs are encoded in the presumptive US4 and US5 loci within US2-US11 region (Supplementary Fig. 1a)[13, 14]. Given that many gene products in the US2-US11 region can block the MHC class I antigen presentation pathway, we hypothesized that some of these miRNAs can inhibit MHC class I-mediated antigen presentation. To identify potential cellular targets of HCMV miRNAs encoded within the US2-US11 region, we investigated changes in the host cell transcriptome in response to the expression of HCMV miRNAs (miR-US4-1, miR-US5-1, and miR-US5-2). We synthesized 3 miRNAs and siRNAs that target green fluorescence protein (GFP) (Control) and protein disulfide isomerase (PDI) (siPDI) as a positive control for evaluating the transfection efficiency. We transfected these synthetic RNAs twice into U373MG cells, an HCMV-permissive cell line[25], at intervals of 48 h to maximize the transfection efficiency. Immunoblotting showed that PDI expression was dramatically reduced in siRNA-PDI-transfected cells (Supplementary Fig. 1b), confirming that the transfection efficiency of miRNAs was sufficient to proceed to the microarray analysis. Microarray analysis for 3 HCMV miRNAs was performed using Agilent Human Whole genome 44K 4Plex arrays. Among the top ranked genes that were most decreased, ERAP1 mRNA was downregulated more than 10-fold by miR-US4-1 (Fig. 1a), whereas miR-US5-1 and miR-US5-2 didn't significantly alter the ERAP1 mRNA level (Fig. 1b, c). Since ERAP1 plays a critical role in regulating the antigenic peptide pool in the ER[4], we investigated whether miR-US4-1 targets ERAP1 to inhibit MHC class I-mediated antigen presentation.

Downregulation of ERAP1 mRNA and protein by miR-US4-1

The human ERAP1 gene produces at least 2 mRNA isoforms, isoform a (ERAP1a) and isoform b (ERAP1b) (Supplementary Fig. 2a). Although the amino acid sequences of both isoforms are almost identical, the 3′-UTR sequence of ERAP1a differs from that of ERAP1b. Because the base-pairing between an miRNA and its target mRNA generally occurs in the 3′-UTR of the target mRNA in animal cells[26], we investigated which of the isoforms was targeted by miR-US4-1. To confirm the microarray data, we expressed control miRNA, miR-US4-1, and siRNAs as positive knockdown controls (siERAP1 which targets ORFs of both isoforms, siERAP1a which targets the 3′-UTR of ERAP1a, and siERAP1b which targets the 3′-UTR of ERAP1b) in human embryonic kidney cell line HEK293T cells as a form of small hairpin RNA (shRNA). We performed quantitative real-time polymerase chain reaction (qRT-PCR) analysis with primers that bind to specific regions in the 3′-UTRs of both isoforms (Supplementary Fig. 2a). As expected, siERAP1a and siERAP1b reduced ERAP1a and ERAP1b mRNA levels respectively, and siERAP1 downregulated both isoforms. ERAP1a mRNA was not downregulated by miR-US4-1 expression (Fig. 1d), while the ERAP1b mRNA level was reduced by more than 60% by miR-US4-1 (Fig. 1e). These results indicate that miR-US4-1 specifically downregulates ERAP1b mRNA but not ERAP1a mRNA.

Next, we determined whether the decrease in the ERAP1b mRNA level led to a decrease in the amount of protein. As a control, we constructed a seed nucleotide (2nd to 8th nucleotides in the 5′-end of the mature miRNA)-mutated miR-US4-1 vector (miR-US4-1(M)) (Supplementary Fig. 2b) because the seed sequence of miRNAs is considered a critical determinant of miRNA-target mRNA recognition and base-pairing, and most miRNAs bind to their target mRNA 3′-UTRs with complete Watson-Crick base-pairing in the seed region[27]. We expressed control miRNA, miR-US4-1, siERAP1, and miR-US4-1(M) in HeLa cells. We investigated the expression of miR-US4-1 using either an RNase protection

assay (RPA) (Fig. 1f, third panel) or northern blot analysis (Fig. 1g, third panel). Immunoblotting showed that ERAP1 protein expression was decreased by miR-US4-1 compared to the control miRNA (Fig. 1f, compare lanes 1 and 2), but miR-US4-1(M) did not affect ERAP1 protein expression (Fig. 1f, lane 4). The ability of miR-US4-1 to downregulate the amount of ERAP1 protein appeared to be as effective as that of siERAP1 (Fig. 1f, compare lanes 2 and 3). ERAP1b mRNA is 3.8–6.4 times more abundant in cells used in these experiments than ERAP1a mRNA (Supplementary Fig. 3a). To rule out the possibility that the direct comparison of ERAP1a and b mRNAs might be biased due to the differential primer efficiency, we validated that both primers amplified each targeted ERAP1 isoform equally (Supplementary Fig. 3b, c). Thus, our findings suggest that ERAP1b protein levels account for most of the ERAP1 contents in the cell. In dose-dependent experiments, the amount of ERAP1 protein was inversely proportional to miR-US4-1 expression (Fig. 1f). These results demonstrate that miR-US4-1 specifically downregulates ERAP1b mRNA levels, thereby reducing the overall cellular ERAP1 protein level.

Direct targeting of ERAP1b mRNA 3′-UTR by miR-US4-1

To confirm whether the reduction of ERAP1b mRNA and ERAP1 protein was due to direct miR-US4-1 targeting and to identify potential target sites in the 3′-UTR of ERAP1 mRNA, we performed bioinformatic scanning of the 3′-UTR of ERAP1a and ERAP1b using RNAhybrid algorithm[28] and Rna22 algorithm[29], focusing on the base-pairing within the seed sequence of the miRNA and its binding energy. We selected the most reliable target site in the 3′-UTR sequences of ERAP1a (Fig. 2a) and ERAP1b mRNA (Fig. 2b), followed by the luciferase reporter assay. Notably, we observed that miR-US4-1 significantly downregulated the expression level of the firefly luciferase fused to the ERAP1b wild-type 3′-UTR, whereas miR-US4-1(M) did not (Fig. 2c). In the reciprocal experiment, in which cells were transfected with the firefly luciferase vector inserted by ERAP1b 3′-UTR mutant, neither wild-type miR-US4-1 nor miR-US4-1(M) had an effect on the expression level of firefly luciferase (Fig. 2c). The expression level of the firefly luciferase vector containing either the wild-type or the mutant ERAP1a 3′-UTR was not affected by wild-type miR-US4-1 or miR-US4-1(M) (Fig. 2c). Considering that the binding ability of miR-US4-1 to ERAP1b (−30.5 kcal/mole, Fig. 2b) is higher than that to ERAP1a (−20.4 kcal/mole, Fig. 2a), the insensitivity of ERAP1a to miR-US4-1 might be attributable to insufficient base-pairing between them.

In addition, we examined the dose-dependent effect of miR-US4-1 on the luciferase reporter comprising ERAP1 3′-UTR derivatives. After validating the dose-dependent expression of miR-US4-1 using northern blot analysis (Supplementary Fig. 4), we transfected pGL3-3′-UTR vectors into these cells and performed a luciferase reporter assay. We observed that the firefly luciferase expression from the vector containing the wild-type ERAP1b 3′-UTR was inversely proportional to the level of miR-US4-1 expression, while the expression of firefly luciferase from the vectors containing the wild-type or mutant ERAP1a 3′-UTR and mutant ERAP1b 3′-UTR was not affected by miR-US4-1 (Fig. 2d). By these observations, we concluded that miR-US4-1 targets only the 3′-UTR of ERAP1b mRNA in a seed region binding-dependent manner but not the 3′-UTR of ERAP1a mRNA.

Physical binding of miR-US4-1 with ERAP1b mRNA in RISC

Although many targets of miRNAs have been established using several target prediction algorithms, these algorithms can occasionally result in false-positive cellular targets. To obtain further evidence for the targeting of miR-US4-1 to ERAP1b, we examined the physical interaction between ERAP1b mRNA and miR-US4-1 using RNA-induced silencing complex (RISC) immunoprecipitation (IP) assay. The RISC IP assay was developed to

extract the Argonaute (AGO)-bound mRNAs targeted by miRNAs[30, 31]. To validate whether the known target mRNAs of a specific miRNA can be enriched using RISC IP assay in our hands, we chose has-miR-21 (miR-21) as a model miRNA of RISC IP assay because human miR-21 is known to have a variety of human target genes, such as *PDCD4, SPRY2, TPM1, MASPIN, RECK*, and *PTEN*[32]. Validating that the sh-miR-21-expressing vector produced the same sequence and size of endogenous miR-21 (pcDNA3.1-miR-21, this vector contains miR-21 pre-miRNA sequence flanked by ~100bp extension of miR-21 pri-miRNA transcript) (Supplementary Fig. 5a), sh-miR-21-expressing vector was co-transfected with each of N-terminally FLAG-tagged human AGO vectors into HEK293T cells. Although human miRNAs can generally complex with any kind of human AGO proteins (hAGO1, hAGO2, hAGO3, and hAGO4) within the RISC (Supplementary Fig. 5b)[33], we used a combination of 4 human AGO genes to exclude the possibility that a specific miRNA targets the specific mRNA with 1 or more AGO proteins. At 48 h post transfection, we validated the expression of FLAG-hAGOs in total cell lysates and the enrichment of FLAG-hAGOs in RISC immunoprecipitates (Supplementary Fig. 5c). As predicted by the results of previous studies[32], all known target mRNAs of miR-21 were enriched under miR-21 overexpression conditions, validating the fidelity of our assay (Supplementary Fig. 5d, e).

Using the same experimental conditions, after confirming the expression and enrichment of miR-US4-1 (Fig. 2e) and FLAG-hAGOs (Fig. 2f) in whole cell lysates and immunoprecipitated samples, we examined the physical interaction of miR-US4-1 with ERAP1b mRNA using qRT-PCR. We found that ERAP1a mRNA enrichment could not be detected in the presence of miR-US4-1 (Fig. 2g). In contrast, ERAP1b mRNA was enriched by about 3.8-fold, solely when miR-US4-1 was over-expressed (Fig. 2h). As expected, neither of the ERAP1 isoforms was enriched when miR-US4-1(M) was expressed (Fig. 2g, h). Together, these results demonstrate that miR-US4-1 physically interacts with ERAP1b mRNA within the RISC complex.

Downregulation of ERAP1 during HCMV infection

We next investigated whether ERAP1 was downregulated by miR-US4-1 during HCMV infection. Because the pre- or mature miRNA sequence of miR-US4-1 is located within the 5′-UTR of putative transcripts encoding US5, a complete deletion of the entire pre-miRNA sequence from the HCMV genome might affect the expression of the neighbor genes near the miR-US4-1 sequence. Thus, to exclude any side effects of full sequence deletion of miR-US4-1 region, we generated an HCMV AD169 mutant (HCMV ΔUS4), in which Drosha processing of the miR-US4-1 primary transcript was defective, by only substituting 6 nucleotides around the predicted cropping site that contains 3 nucleotides of the 5′-end of the mature miR-US4-1 (Supplementary Fig. 6). To validate that an intact virus was generated without disrupting the entire HCMV genome, we constructed a control revertant virus (HCMV REV), whose genome sequence was theoretically identical to that of wild type HCMV (HCMV WT) using HCMV ΔUS4 as a template. HCMV WT, ΔUS4, and REV viruses were infected into human foreskin fibroblast (HFF) cells followed by RPA to analyze the miR-US4-1 expression. In both HCMV WT and REV infections, the expression of miR-US4-1 began at about 24 h post infection and increased until 72 h post infection, whereas miR-US4-1 was not expressed in HCMV ΔUS4-infected HFF cells (Fig. 3a). Immunoblot of the infected cell lysates revealed that the overall amount of ERAP1 protein decreased upon HCMV WT and REV infection, while they remained unchanged in HCMV ΔUS4-infected cells (Fig. 3b, first panel). The miR-US4-1 expression did not affect the expression of irrelevant targets immediate early 1 and 2 (IE1/2) or GAPDH (Fig. 3b, second and third panels), indicating a specific effect of miR-US4-1 on ERAP1 expression.

We next analyzed the alteration in the mRNA level of ERAP1 isoforms during the course of infection. No detectable difference in the levels of ERAP1a mRNA was observed between

HCMV WT and ΔUS4 throughout the course of infection (Supplementary Fig. 7a). While HCMV ΔUS4 infection had little effect on ERAP1b mRNA levels, the ERAP1b mRNA level was decreased by HCMV WT infection and reached about 10% of that seen in uninfected HFF at 72 h post infection. The miR-US4-1 expression did not affect the expression of IE1 mRNA (Supplementary Fig. 7b), indicating a specific effect of miR-US4-1 on ERAP1b mRNA expression. These results suggest that the downregulation of ERAP1 protein primarily resulted from miR-US4-1-mediated downregulation of ERAP1b mRNA.

Inhibition of ovalbumin precursor trimming by miR-US4-1

As part of the effort to determine the biological relevance of miR-US4-1, we initially assessed the effect of miR-US4-1 on the production of the SIINFEKL peptide (referred to as OVA8, and generated from amino acids 257–264 of ovalbumin) from an ovalbumin-derived precursor by using the well-known OVA8 experimental system[5, 29]. Using mouse H-2K^b-expressing HeLa (HeLa-K^b) cells, we cotransfected pUG1 vectors encoding OVA8 or the 13-amino acid peptide LEQLESIINFEKL (N5OVA8) with miRNA or siRNA. Given that the peptide was fused to the C-terminal end of ubiquitin to allow for post-translational cleavage of the peptide from cytosolic ubiquitin by ubiquitin C-terminal hydrolase[34] and ERAP1 can trim N5OVA8 precursor to mature OVA8 peptide[29], we monitored the generation of OVA8 by measuring the B3Z 86/90.14 (B3Z) T cell hybridoma response. Since B3Z T cells are a CD8$^+$ T cell hybridoma line generated by fusing the OVA-Kb-specific cytotoxic clone B3 with a lacZ-inducible derivative of BW5147 and engineered to secrete β-galactosidase when its T cell receptor engages an H-2K^b-OVA8 complex[35, 36], the B3Z T cell response can be measured by quantifying β-galactosidase production.

Validating the specific and sufficient knockdown of ERAP1b mRNA by miR-US4-1 to the level of that seen in siERAP1 treated cells (Fig. 4a), we found that miR-US4-1 expression led to a reduced B3Z response compared to control miRNA expression in N5OVA8-expressing HeLa-K^b cells (Fig. 4b). The miR-US4-1(M) failed to reduce the B3Z response, while siERAP1 as a control was competent to inhibit the B3Z response (Fig. 4b). In a control experiment, we observed that miR-US4-1, siERAP1, or miR-US4-1(M) had no effect on B3Z responses in OVA8-expressing cells (Fig. 4c). In addition, the expression of miR-US4-1 did not affect the steady-state level of components of the MHC class I antigen presentation machinery, such as MHC class I heavy chain, ERp57, PDI, and Tapasin (Supplementary Fig. 8). In accordance with previous observations in the ERAP1 knock-out (KO) mice[34, 37, 38], our findings indicate that miR-US4-1 is able to inhibit trimming of the OVA8 precursor to OVA8 mature peptide by targeting ERAP1.

Subversion of HCMV-specific CTL response by miR-US4-1

To directly demonstrate the physiological significance of miR-US4-1, we proceeded to perform CTL assays in the presence or absence of miR-US4-1 in the context of HCMV infection, using CD8$^+$ HCMV-specific CTLs clones from HCMV-seropositive donors (Table 1). Initially, we examined whether ERAP1 is involved in the generation of HCMV-derived CTL epitopes using an *in vitro* ERAP1 trimming assay. The 2 amino acid N-terminally extended form of the synthetic peptide precursor was incubated with various amounts of recombinant ERAP1. The generation of mature epitopes was monitored by analytical high performance liquid chromatography (HPLC) (Fig. 5a), and the rate of mature epitope generation was calculated (Table 1). All precursors tested (UL23$_{34–42}$, IE1$_{88–96}$, UL28$_{327–335}$, UL16$_{162–170}$, and UL105$_{715–723}$) were effectively trimmed to their mature epitopes. In the case of UL105$_{715–723}$, the rate of mature epitope generation was relatively slow compared to that of other epitopes and was further trimmed to short peptides by

ERAP1 (Fig. 5a). These *in vitro* results suggest that ERAP1 can be involved in the generation of a broad spectrum of HCMV epitopes.

HCMV AD169 WT possesses several immune evasion proteins in the US2-US11 region that downregulate the cell surface expression of MHC class I molecules[1]. To overcome the limitations imposed by these immune evasion proteins and to test the exclusive effect of miR-US4-1 on CTL response, we used an HCMV RV798 strain deleted of the US2-US11 genome region including miR-US4-1. HCMV RV798 infection, unlike HCMV AD169 WT and AD169 ΔUS4, slightly up-regulated the surface expression of MHC class I molecules (Supplementary Fig. 9). Autologous fibroblasts were transfected with synthetic miR-US4-1 twice prior to infection. At 24 h after the second transfection, we infected fibroblast cells with HCMV RV798 and validated the expression of viral genes that encode the viral protein containing epitopes used in the *in vitro* ERAP1 trimming assay by RT-PCR analysis (Supplementary Fig. 10). The efficiency of ERAP1b knockdown by miR-US4-1 was up to 65–80% in all donor fibroblasts at 48 h post infection (Supplementary Fig. 11). The miR-US4-1-mediated knockdown of ERAP1 inhibited the lysis of antigen-specific target cells by 5 CTL clones 1B12-24, 1F8-68, 2A1-3, 1A4-1, and 9G4-107 (Fig. 5b). The CTL clone IA8-8 specific to $UL105_{715–723}$ epitope was efficiently able to lyse the target cells regardless of ERAP1 activity (Fig. 5b), not all HCMV epitopes are generated in an ERAP1-dependent manner. Overall, these data provide direct evidence for a critical role of miR-US4-1 in immune evasion from CTL responses by targeting ERAP1, a key component of the antigen processing machinery. Furthermore, our work supports an important *in vivo* role of ERAP1 in antiviral CTL immune responses in humans.

Discussion

In this study, we showed that HCMV miR-US4-1 targets ERAP1b mRNA but not to ERAP1a, resulting in the downregulation of overall ERAP1 protein. We also revealed that miR-US4-1 specifically bound to ERAP1b mRNA within the RISC complex, and the 3′-UTR of ERAP1b mRNA was targeted by miR-US4-1 in a manner that destabilized or degraded mRNA and eventually lead to a decrease in the ERAP1b mRNA level. We demonstrated that during HCMV infection, ERAP1b mRNA level and overall ERAP1 protein expression were inversely proportional to the miR-US4-1 expression. Furthermore, we demonstrated that miR-US4-1 inhibited the lysis of infected target cells by CTLs, providing evidence of its physiological relevance. Thus, our results reveal a novel miRNA-based immune evasion strategy in which miR-US4-1 interferes with MHC class I-mediated antigen presentation by targeting ERAP1, a key enzyme involved in catalyzing the production of antigenic peptides in the ER.

ERAP1 is critical in establishing immune responses to some viral epitopes. ERAP1 deficiency in mice affects the peptide pool during mouse CMV[39] and lymphocytic choriomeningitis virus (LCMV)[37] infection as well as $CD8^+$ T cell responses for LCMV-derived[38] or influenza virus-derived[37] antigens. In ERAP1-KO mice, many unstable, likely N-terminally extended MHC class I-bound peptides are presented to the cell surface[8]. In our experiments using HCMV-specific $CD8^+$ CTL clones derived from HCMV-seropositive donors, we found that the generation of 4 epitopes ($UL23_{34–42}$, $IE1_{88–96}$, $UL28_{327–335}$, and $UL16_{162–170}$) among 5 HCMV epitopes tested was affected by ERAP1. Based on previous studies in ERAP1-KO mice and our current findings, we conclude that ERAP1 downregulation influences the production of many HCMV-derived antigenic peptides in viral infection, resulting in evasion of viral antigen recognition by $CD8^+$ T cells during the host immune response.

In addition to ERAP1, human cells express 2 additional aminopeptidases that are involved in antigenic peptide processing, i.e., ER aminopeptidase 2 (ERAP2, also known as L-RAP) and placental leucine aminopeptidase (PLAP, also known as IRAP). ERAP2 can efficiently trim some kinds of epitopes that are distinct from ERAP1-trimmed epitopes[40], and it can physically bind to ERAP1[6], suggesting that ERAP1 and ERAP2 might function in a concerted manner to produce a variety of MHC class I epitopes in the ER. However, not only is ERAP1 expressed more ubiquitously than ERAP2, but its overall expression level is higher than ERAP2 in human cell lines[6, 41]. In addition, although PLAP can produce distinct antigenic peptides, it is specialized to localize to intracellular vesicles[42]. Therefore, ERAP1 appears to be a major trimming enzyme of antigenic peptides in the ER of human cells. In this regard, it is plausible that HCMV has evolved a strategy to preferentially target ERAP1 rather than other aminopeptidases to inhibit the presentation of epitopes derived from viral gene products under the selective pressure of the host immune response. Of course, it is still possible that the expression or function of ERAP2 and PLAP might also be regulated by HCMV or other viruses for their survival.

It is crucial for viral survival to block the presentation of viral antigenic peptides to $CD8^+$ T cells at immediate early (IE) or early (E) stages of infection. The US2-US11 region of the HCMV genome encodes immune evasion proteins that can inhibit MHC class I antigen presentation[1]. The physiological importance of the US2-US11 region has been highlighted by a recent finding that superinfection of rhesus CMV-infected rhesus macaques requires evasion of $CD8^+$ T cell immunity by the homologs of HCMV US2, 3, 6, and 11[43]. Given that miR-US4 is co-expressed with these immune evasion proteins at the E stage, miR-US4 is likely to act cooperatively and simultaneously with these immune evasion proteins for immune evasion. Unlike these US glycoproteins, viral miRNAs are non-immunogenic, and thus viral miRNAs might offer better options for viruses to enable them to establish a lifelong latent infection. This work should expand the scope of CTL immunoevasive gene products beyond viral glycoproteins to viral miRNAs. Identifying cooperation between viral miRNA and viral proteins in immune evasion underscores the necessity to incorporate additional determinants in HCMV vaccine design.

Supplementary Material

Refer to Web version on PubMed Central for supplementary material.

Acknowledgments

We thank Masafumi Tsujimoto for providing recombinant human ERAP1 cDNA and the anti-ERAP1 polyclonal antibody, Peter van Endert and Loredana Saveanu for providing the anti-ERAP1 monoclonal antibody 6H9, Ian York and Kenneth Rock for providing pUG1-based vectors and technical help, Nilabh Shastri for providing B3Z T cell hybridoma, Thomas Shenk for pAD/Cre BAC and Chang-Yuil Kang and Tae-Kyu Kim for technical help. This work was supported by the Creative Research Initiative Program (K.A.) and by BK21 Research Fellowships (S.K., S.L. and D.K.) from the Ministry of Education, Science and Technology of the Republic of Korea and by NIH CA18029 and AI053193 (S.R.R).

References

1. Hansen TH, Bouvier M. MHC class I antigen presentation: learning from viral evasion strategies. Nat Rev Immunol. 2009; 9:503–513. [PubMed: 19498380]
2. Vyas JM, Van der Veen AG, Ploegh HL. The known unknowns of antigen processing and presentation. Nat Rev Immunol. 2008; 8:607–618. [PubMed: 18641646]
3. Nguyen TT, et al. Structural basis for antigenic peptide precursor processing by the endoplasmic reticulum aminopeptidase ERAP1. Nat Struct Mol Biol. 2011; 18:604–613. [PubMed: 21478864]
4. Haroon N, Inman RD. Endoplasmic reticulum aminopeptidases: Biology and pathogenic potential. Nat Rev Rheumatol. 2010; 6:461–467. [PubMed: 20531381]

5. Saric T, et al. An IFN-gamma-induced aminopeptidase in the ER, ERAP1, trims precursors to MHC class I-presented peptides. Nat Immunol. 2002; 3:1169–1176. [PubMed: 12436109]
6. Saveanu L, et al. Concerted peptide trimming by human ERAP1 and ERAP2 aminopeptidase complexes in the endoplasmic reticulum. Nat Immunol. 2005; 6:689–697. [PubMed: 15908954]
7. Kanaseki T, Shastri N. Endoplasmic reticulum aminopeptidase associated with antigen processing regulates quality of processed peptides presented by MHC class I molecules. J Immunol. 2008; 181:6275–6282. [PubMed: 18941218]
8. Hammer GE, Gonzalez F, James E, Nolla H, Shastri N. In the absence of aminopeptidase ERAAP, MHC class I molecules present many unstable and highly immunogenic peptides. Nat Immunol. 2007; 8:101–108. [PubMed: 17128277]
9. Chang SC, Momburg F, Bhutani N, Goldberg AL. The ER aminopeptidase, ERAP1, trims precursors to lengths of MHC class I peptides by a "molecular ruler" mechanism. Proc Natl Acad Sci U S A. 2005; 102:17107–17112. [PubMed: 16286653]
10. Fabian MR, Sonenberg N, Filipowicz W. Regulation of mRNA translation and stability by microRNAs. Annu Rev Biochem. 2010; 79:351–379. [PubMed: 20533884]
11. Pfeffer S, et al. Identification of virus-encoded microRNAs. Science. 2004; 304:734–736. [PubMed: 15118162]
12. Cullen BR. Viral and cellular messenger RNA targets of viral microRNAs. Nature. 2009; 457:421–425. [PubMed: 19158788]
13. Pfeffer S, et al. Identification of microRNAs of the herpesvirus family. Nat Methods. 2005; 2:269–276. [PubMed: 15782219]
14. Grey F, et al. Identification and characterization of human cytomegalovirus-encoded microRNAs. J Virol. 2005; 79:12095–12099. [PubMed: 16140786]
15. Grey F, Meyers H, White EA, Spector DH, Nelson J. A human cytomegalovirus-encoded microRNA regulates expression of multiple viral genes involved in replication. PLoS Pathog. 2007; 3:e163. [PubMed: 17983268]
16. Grey F, et al. A viral microRNA down-regulates multiple cell cycle genes through mRNA 5'UTRs. PLoS Pathog. 2010; 6 e1000967.
17. Stern-Ginossar N, et al. Host immune system gene targeting by a viral miRNA. Science. 2007; 317:376–381. [PubMed: 17641203]
18. Stern-Ginossar N, et al. Analysis of human cytomegalovirus-encoded microRNA activity during infection. J Virol. 2009; 83:10684–10693. [PubMed: 19656885]
19. Rehm A, et al. Human cytomegalovirus gene products US2 and US11 differ in their ability to attack major histocompatibility class I heavy chains in dendritic cells. J Virol. 2002; 76:5043–5050. [PubMed: 11967320]
20. Machold RP, Wiertz EJ, Jones TR, Ploegh HL. The HCMV gene products US11 and US2 differ in their ability to attack allelic forms of murine major histocompatibility complex (MHC) class I heavy chains. J Exp Med. 1997; 185:363–366. [PubMed: 9016885]
21. Gruhler A, Peterson PA, Fruh K. Human cytomegalovirus immediate early glycoprotein US3 retains MHC class I molecules by transient association. Traffic. 2000; 1:318–325. [PubMed: 11208117]
22. Lehner PJ, Karttunen JT, Wilkinson GW, Cresswell P. The human cytomegalovirus US6 glycoprotein inhibits transporter associated with antigen processing-dependent peptide translocation. Proc Natl Acad Sci U S A. 1997; 94:6904–6909. [PubMed: 9192664]
23. Park B, Spooner E, Houser BL, Strominger JL, Ploegh HL. The HCMV membrane glycoprotein US10 selectively targets HLA-G for degradation. J Exp Med. 2010; 207:2033–2041. [PubMed: 20713594]
24. Gustems M, et al. Regulation of the transcription and replication cycle of human cytomegalovirus is insensitive to genetic elimination of the cognate NF-kappa B binding sites in the enhancer. Journal of Virology. 2006; 80:9899–9904. [PubMed: 16973595]
25. Wu J, O'Neill J, Barbosa MS. Transcription factor Sp1 mediates cell-specific trans-activation of the human cytomegalovirus DNA polymerase gene promoter by immediate-early protein IE86 in glioblastoma U373MG cells. J Virol. 1998; 72:236–244. [PubMed: 9420220]

26. Chekulaeva M, Filipowicz W. Mechanisms of miRNA-mediated post-transcriptional regulation in animal cells. Curr Opin Cell Biol. 2009; 21:452–460. [PubMed: 19450959]
27. Lewis BP, Burge CB, Bartel DP. Conserved seed pairing, often flanked by adenosines, indicates that thousands of human genes are microRNA targets. Cell. 2005; 120:15–20. [PubMed: 15652477]
28. Rehmsmeier M, Steffen P, Hochsmann M, Giegerich R. Fast and effective prediction of microRNA/target duplexes. RNA. 2004; 10:1507–1517. [PubMed: 15383676]
29. Miranda KC, et al. A pattern-based method for the identification of MicroRNA binding sites and their corresponding heteroduplexes. Cell. 2006; 126:1203–1217. [PubMed: 16990141]
30. Wang WX, Wilfred BR, Hu Y, Stromberg AJ, Nelson PT. Anti-Argonaute RIP-Chip shows that miRNA transfections alter global patterns of mRNA recruitment to microribonucleoprotein complexes. RNA. 2010; 16:394–404. [PubMed: 20042474]
31. Nonne N, Ameyar-Zazoua M, Souidi M, Harel-Bellan A. Tandem affinity purification of miRNA target mRNAs (TAP-Tar). Nucleic Acids Res. 2010; 38:e20. [PubMed: 19955234]
32. Moore LM, Zhang W. Targeting miR-21 in glioma: a small RNA with big potential. Expert Opin Ther Targets. 2010; 14:1247–1257. [PubMed: 20942748]
33. Peters L, Meister G. Argonaute proteins: mediators of RNA silencing. Mol Cell. 2007; 26:611–623. [PubMed: 17560368]
34. York IA, Brehm MA, Zendzian S, Towne CF, Rock KL. Endoplasmic reticulum aminopeptidase 1 (ERAP1) trims MHC class I-presented peptides in vivo and plays an important role in immunodominance. Proc Natl Acad Sci U S A. 2006; 103:9202–9207. [PubMed: 16754858]
35. Karttunen J, Sanderson S, Shastri N. Detection of rare antigen-presenting cells by the lacZ T-cell activation assay suggests an expression cloning strategy for T-cell antigens. Proc Natl Acad Sci U S A. 1992; 89:6020–6024. [PubMed: 1378619]
36. Shastri N, Gonzalez F. Endogenous generation and presentation of the ovalbumin peptide/Kb complex to T cells. J Immunol. 1993; 150:2724–2736. [PubMed: 8454852]
37. Firat E, et al. The role of endoplasmic reticulum-associated aminopeptidase 1 in immunity to infection and in cross-presentation. J Immunol. 2007; 178:2241–2248. [PubMed: 17277129]
38. Yan J, et al. In vivo role of ER-associated peptidase activity in tailoring peptides for presentation by MHC class Ia and class Ib molecules. J Exp Med. 2006; 203:647–659. [PubMed: 16505142]
39. Blanchard N, et al. Endoplasmic reticulum aminopeptidase associated with antigen processing defines the composition and structure of MHC class I peptide repertoire in normal and virus-infected cells. J Immunol. 2010; 184:3033–3042. [PubMed: 20173027]
40. Tanioka T, et al. Human leukocyte-derived arginine aminopeptidase. The third member of the oxytocinase subfamily of aminopeptidases. J Biol Chem. 2003; 278:32275–32283. [PubMed: 12799365]
41. Fruci D, et al. Altered expression of endoplasmic reticulum aminopeptidases ERAP1 and ERAP2 in transformed non-lymphoid human tissues. J Cell Physiol. 2008; 216:742–749. [PubMed: 18393273]
42. Georgiadou D, et al. Placental leucine aminopeptidase efficiently generates mature antigenic peptides in vitro but in patterns distinct from endoplasmic reticulum aminopeptidase 1. J Immunol. 2010; 185:1584–1592. [PubMed: 20592285]
43. Hansen SG, et al. Evasion of CD8+ T cells is critical for superinfection by cytomegalovirus. Science. 2010; 328:102–106. [PubMed: 20360110]
44. Manley TJ, et al. Immune evasion proteins of human cytomegalovirus do not prevent a diverse CD8+ cytotoxic T-cell response in natural infection. Blood. 2004; 104:1075–1082. [PubMed: 15039282]
45. Evnouchidou I, et al. The internal sequence of the peptide-substrate determines its N-terminus trimming by ERAP1. PLoS One. 2008; 3:e3658. [PubMed: 18987748]
46. Niles AL, Moravec RA, Riss TL. In vitro viability and cytotoxicity testing and same-well multi-parametric combinations for high throughput screening. Curr Chem Genomics. 2009; 3:33–41. [PubMed: 20161834]
47. Lee Y, et al. The nuclear RNase III Drosha initiates microRNA processing. Nature. 2003; 425:415–419. [PubMed: 14508493]

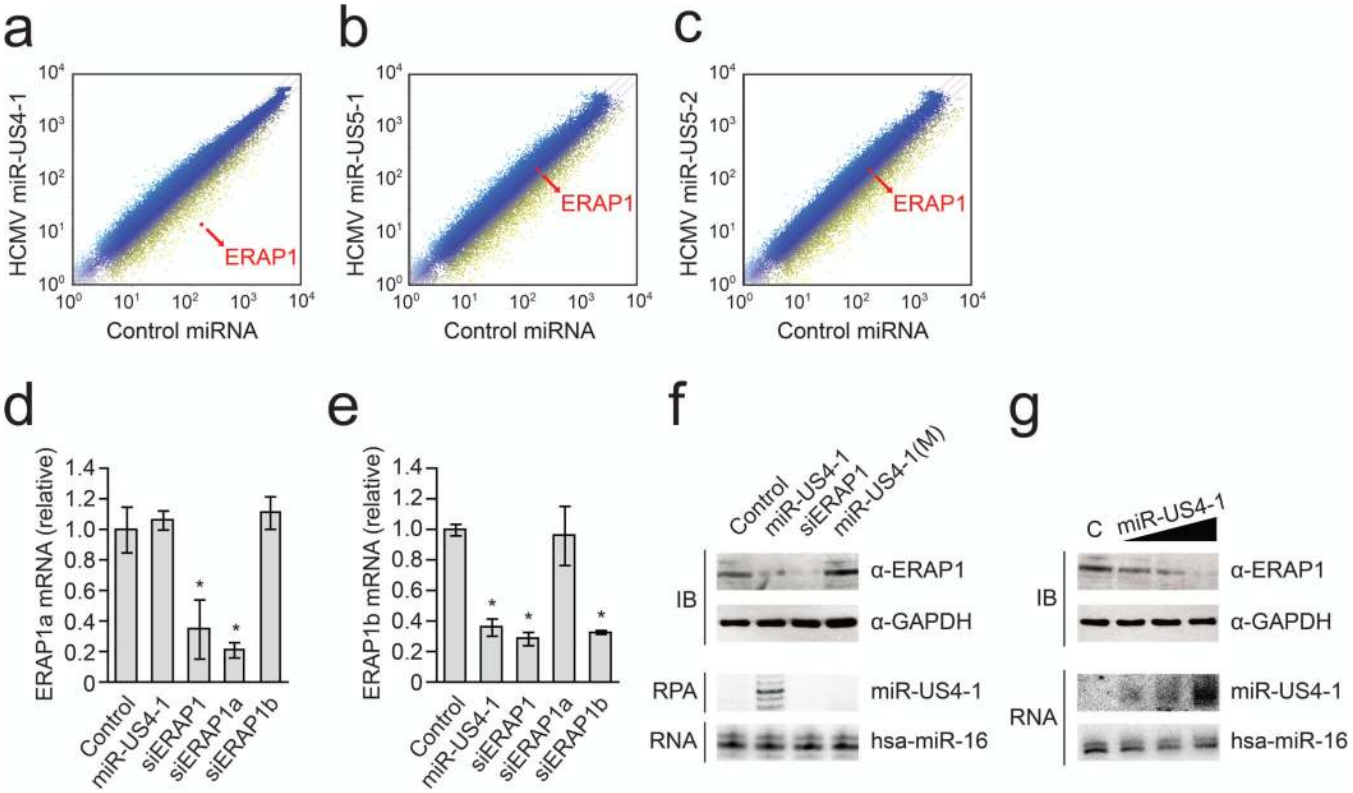

Figure 1. The mRNA level and protein of ERAP1 isoform b but not ERAP1 isoform a are reduced by HCMV miR-US4-1 expression

(**a, b, c**) Relative change in cellular mRNA levels by viral miRNAs (**a**, miR-US4-1; **b**, miR-US5-1; **c**, miR-US5-2) compared to control miRNA (siRNA-GFP). The expression level of ERAP1 is indicated with a red dot. (**d, e**) The expression levels of (**d**) ERAP1a and (**e**) ERAP1b mRNA were analyzed using qRT-PCR and normalized to GAPDH (glyceraldehyde 3-phosphate dehydrogenase). *P < 0.05, two-tailed Student's t-test compared with control miRNA. Data are presented "relative" to the value of GAPDH as means ± s.d., n = 3. (**f**) HEK293T cells were transfected with 10 μg of pSuperRetro vectors, siGFP as control miRNA, miR-US4-1, siERAP1, and miR-US4-1(M), followed by selection with 2 μg puromycin for 1 week. (**g**) HEK293T cells were transfected with different concentrations of pSuperRetro-miR-US4-1 vector (2 μg, 4 μg, and 10 μg in lanes 2, 3, and 4, respectively). (**f, g**) The expression level of the ERAP1 protein was analyzed by immunoblot, with GAPDH as a protein loading control. The expression level of miR-US4-1 was analyzed by (**f**) RNase protection assay (RPA) or (**g**) RNA blot analysis. Hsa-miR-16 served as an RNA loading control. Data are representative of 3 independent experiments. C, control miRNA.

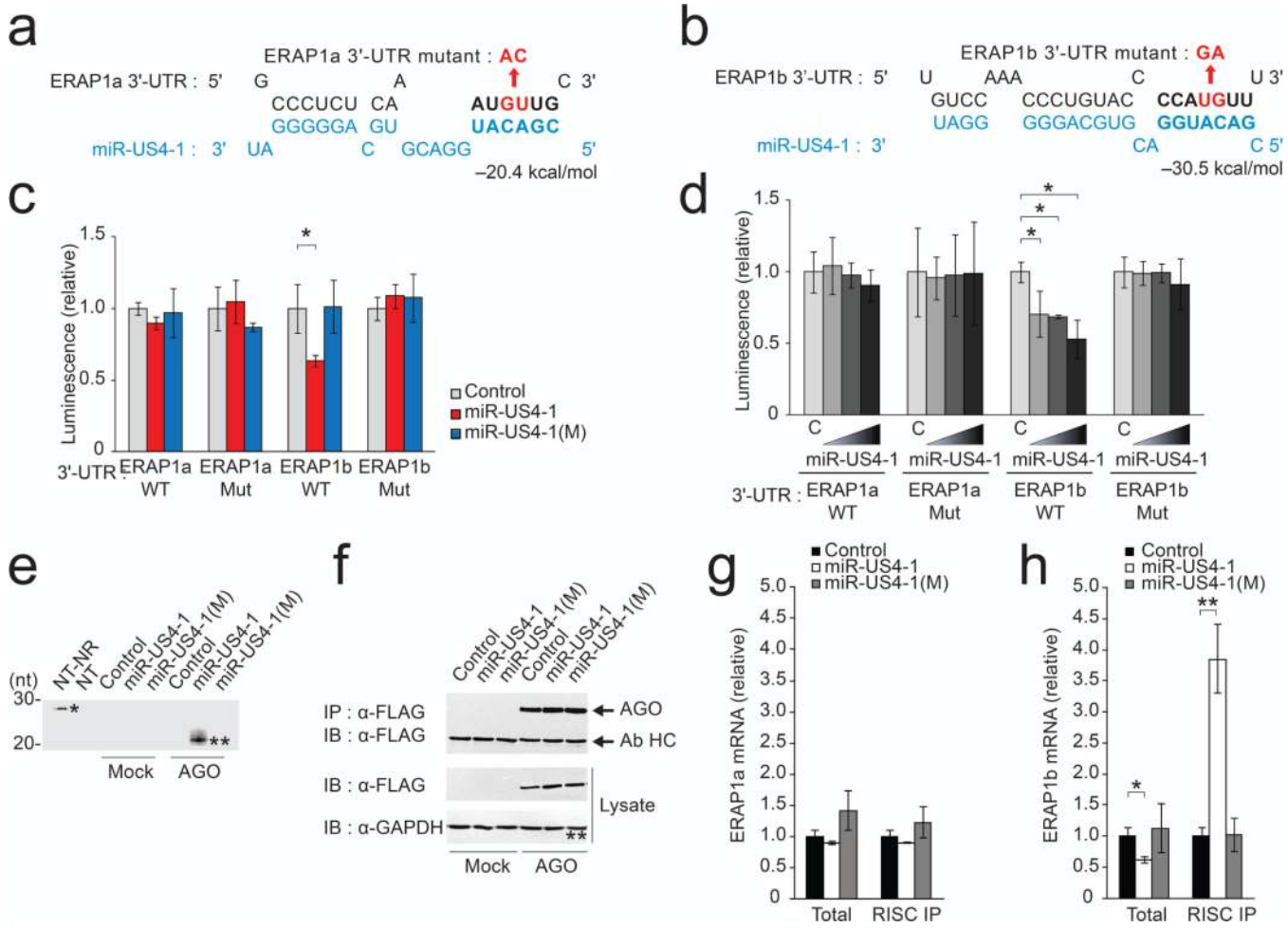

Figure 2. HCMV miR-US4-1 targets the 3′-UTR of ERAP1 isoform b and physically binds to ERAP1 isoform b mRNA within the RISC

Predicted binding site of the 3′-UTR of ERAP1a mRNA (**a**) and ERAP1b mRNA (**b**) by miR-US4-1. Bold characters indicate the expected seed region interaction site. The nucleotide sequence in red was replaced with the sequence indicated by the arrow in mutant 3′-UTRs. The HCMV miR-US4-1 sequence is shown in blue. (**c**) Dual luciferase assays were performed in HEK293T cells using 5 μg of the miRNA-expressing vector, 10 ng of the pGL3-3′-UTR-containing vector, and 5 ng of the Renilla control vector. (**d**) A dual luciferase assay was performed under the same conditions as in (**c**), except for the use of 1 μg, 2 μg, or 5 μg of the miR-US4-1-expressing vector and 5 μg of the control miRNA-expressing vector. C, control miRNA. (**c, d**) *P < 0.05, two-tailed Student's t-test compared with control miRNA. Data are presented by the luminescence of firefly luciferase "relative" to the luminescence of Renilla luciferase as means ± s.d., n = 3, and are representative of 3 independent experiments. (**e**) HEK293T cells were transfected with the mix of pSuperRetro vectors indicated and empty (Mock) or N-terminally FLAG-tagged human AGO1, 2, 3, and 4 (AGO) vectors. RISC IP was performed at 48 h after transfection. Total RNA was extracted from RISC IP samples, and an RPA was performed to detect miR-US4-1. NT-NR indicates no target-no RNase that the sample did not contain either extracted total RNA or RNase A/T1. NT indicates no target that the sample did not contain extracted total RNA. *Undigested probe, **HCMV miR-US4-1. (**f**) Aliquots of RISC immunoprecipitates and cell lysates were probed with anti-FLAG Ab to confirm the IP and expression of FLAG-

AGOs. (**g, h**) Using RNA extracted from immunoprecipitated RISC or total sample, qRT-PCR was performed to compare the levels of ERAP1a (**g**) and ERAP1b mRNA (**h**). The level of ERAP1 mRNA was normalized to the GAPDH level. *P < 0.05, **P < 0.01, two-tailed Student's t-test compared with control miRNA. Data are presented "relative" to the value of GAPDH as means ± s.d., n = 3, and are representative of 3 independent experiments.

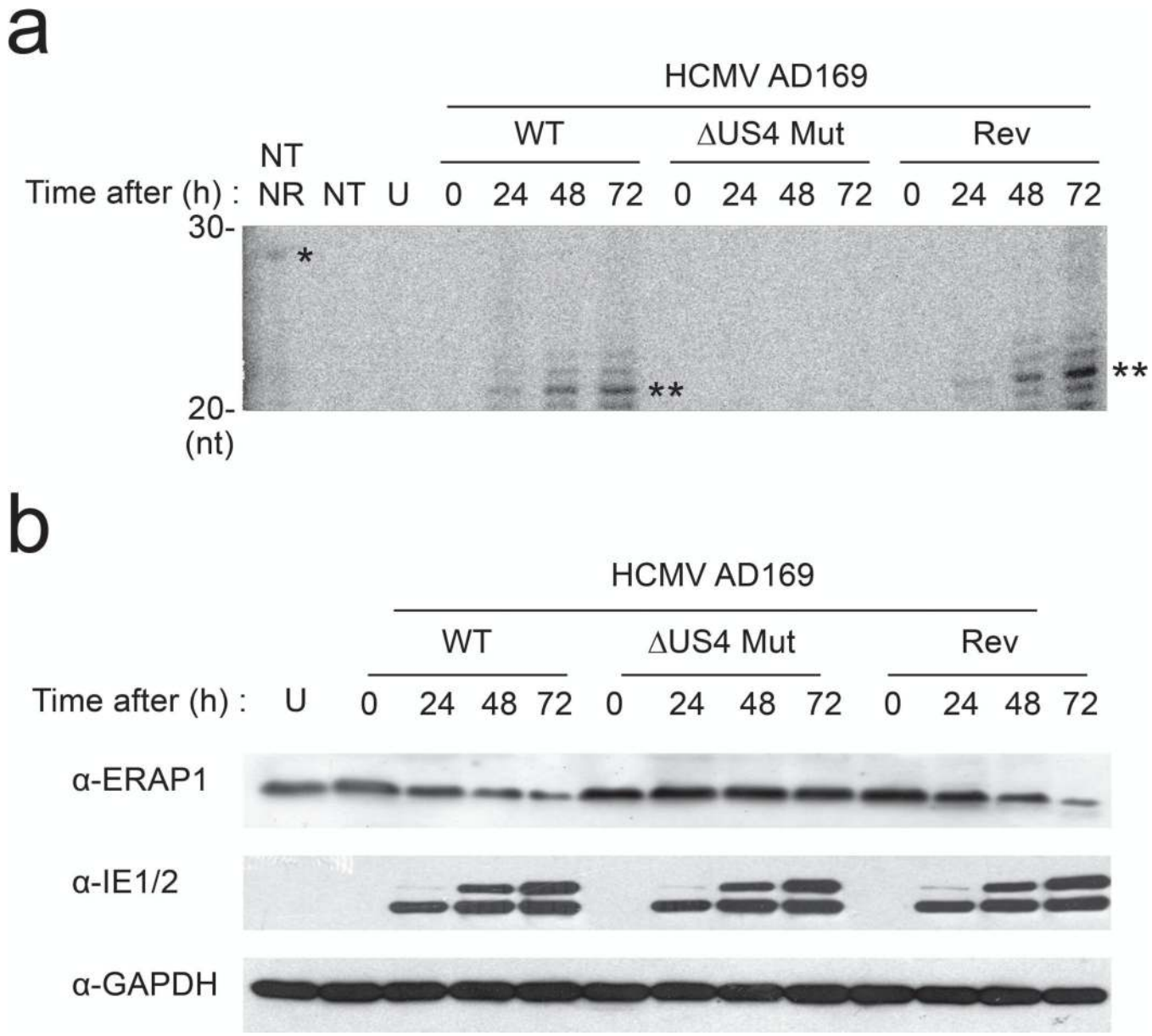

Figure 3. ERAP1 is downregulated in HCMV-infected cells

(**a**) HFF cells were infected with wild-type HCMV AD169, the ΔUS4 mutant, or the revertant for 1 h at MOI = 5. The total RNA was extracted at 0 h, 24 h, 48 h, and 72 h post infection from infected cells or uninfected cells. An RPA was performed to analyze the level of miR-US4-1. NT-NR, no target-no RNase that the sample did not contain either extracted total RNA or RNase A/T1. NT, no target that the sample did not contain extracted total RNA. *Undigested probe, **HCMV miR-US4-1. (**b**) Using the cell aliquots from the samples in **(a)** immunoblot analysis to determine changes in the protein amount of ERAP1, IE1/2, and GAPDH at each post infection time. GAPDH served as protein loading control. Data are representative of 3 independent experiments. U, uninfected. WT, wild type. Mut, mutant. Rev, revertant.

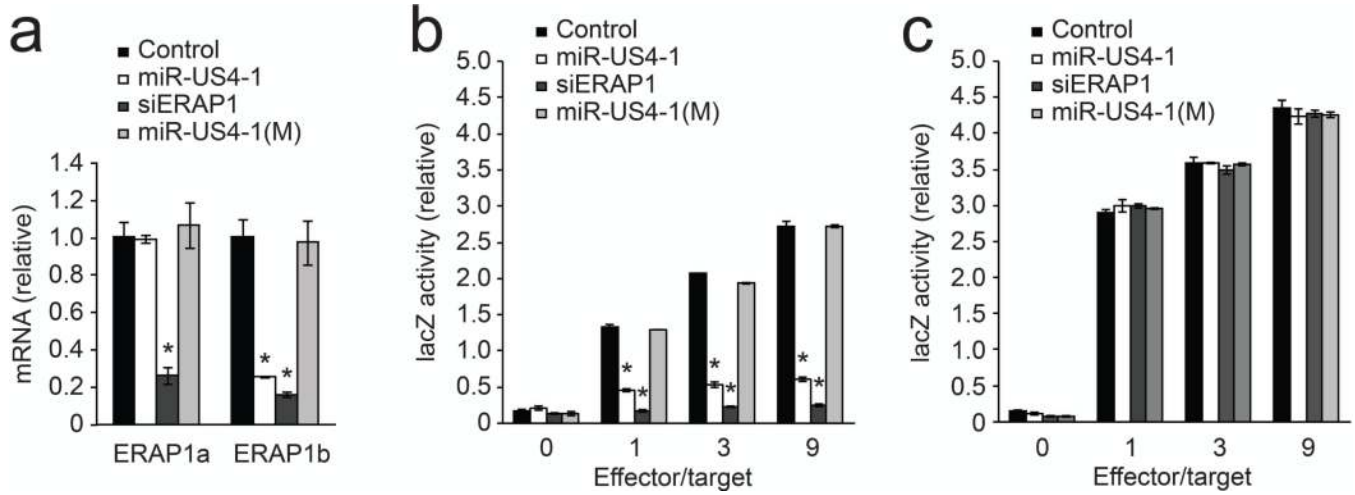

Figure 4. HCMV miR-US4 inhibits the trimming of $Ova_{257–264}$ peptide from ovalbumin precursor peptide by ERAP1

(**a**) H-2K^b-expressing HeLa cells were transfected with control miRNA, miR-US4-1, siERAP1, or miR-US4-1(M). After 1 week of selection with puromycin, the expression levels of ERAP1a and ERAP1b mRNA were analyzed using qRT-PCR and normalized to GAPDH. *P < 0.05, two-tailed Student's t-test compared with control miRNA. Data are presented "relative" to the value of GAPDH as means ± s.d., n = 3, and are representative of 3 independent experiments. (**b, c**) H-2K^b-expressing HeLa cells were transfected with control miRNA, miR-US4-1, siERAP1, or miR-US4-1(M). After 1 week of selection with puromycin, the pUG1-N5OVA8 vector (**b**) or the pUG1-OVA8 vector (**c**) were transfected. After 48 h, 1.0×10^4 transfected H-2K^b-expressing HeLa cells were co-cultured with 1.0×10^4 (1), 3.0×10^4 (3), or 9.0×10^4 (9) B3Z cells. After 16 h incubation, cells were harvested. The lacZ activity was calculated by measuring β-galactosidase production with the lacZ substrate CPRG and presented in graphs as the "relative" levels compared to control miRNA. *P < 0.001, two-tailed Student's t-test compared with control miRNA. Data are presented as means ± s.e.m. of 3 independent experiments.

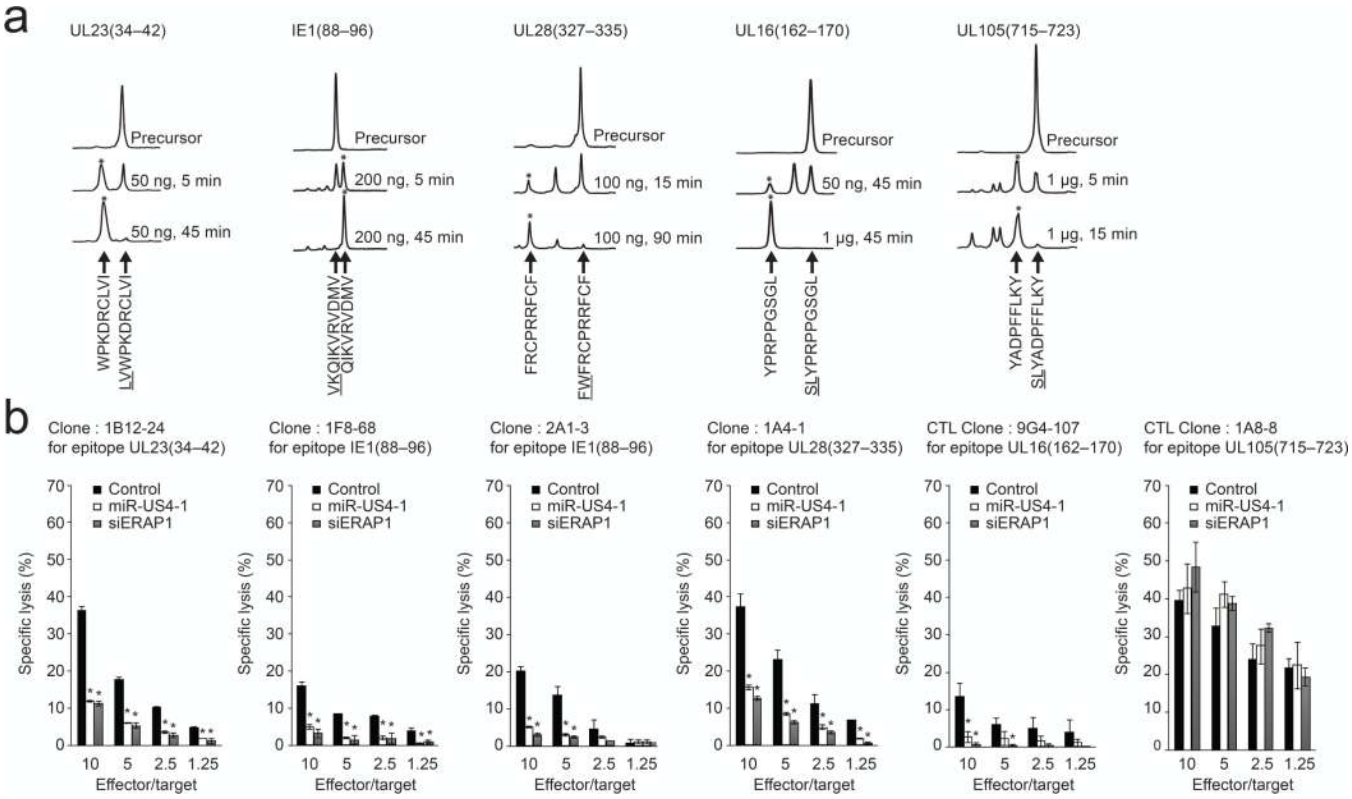

Figure 5. HCMV miR-US4-1 inhibits the generation of HCMV-derived antigenic peptides and the CD8$^+$ CTL responses

(**a**) Characteristic chromatograms indicating epitope production *in vitro* by ERAP1. For each epitope precursor 3 chromatograms are depicted: Top, precursor alone; Middle, precursor incubated with a moderate amount of enzyme; and Bottom, precursor incubated with a larger amount of enzyme. In each case, the peak that corresponds to the mature epitope is indicated by an asterisk. Reaction conditions are indicated next to each chromatogram. The N-terminally extended 2 amino acid sequence within each precursor is underlined. (**b**) For the Chromium release assay, autologous fibroblasts were transfected twice with control miRNA, miR-US4-1, or siERAP1 RNA duplex. After 24 h, cells were infected with HCMV RV798 at MOI = 2 for 1 h. At 48 h post infection, cells were collected and incubated with ^{51}Cr for 2 h in a 37°C CO_2 incubator. These cells were washed and used as target cells. 1.0×10^4 target cells were co-incubated with 1.0×10^5 (10), 5.0×10^4 (5), 2.5×10^4 (2.5), or 1.25×10^4 (1.25) CTLs, of which the clone names are presented above each panel, as effector cells for 6 h in a 37°C CO_2 incubator. The released ^{51}Cr level was measured by γ-irradiation counting. The level of specific CTL lysis was calculated by the following formula: ([specific release - spontaneous release] / [total release - spontaneous release]) × 100 (%). A spontaneous release of less than about 5% of the total release was observed in all assays. *$P < 0.001$, two-tailed Student's t-test compared with control miRNA. Data are presented as means ± s.e.m. of 3 independent experiments.

Table 1

Data collection relationships in the *in vitro* ERAP1 trimming assay and the CTL assay

CTL clone	HCMV Epitope	Mature epitope	Precursor epitope	Generation rate (mol/mol·sec)	Restricted HLA allele	Fibroblast Donor	ERAP1 dependency of CTL response
1B12-24	$UL23_{34–42}$	WPKDRCLVI	**LV**WPKDRCLVI	12.000	B*5101	RT	+
1F8-68	$IE1_{88–96}$	QIKVRVDMV	**VK**QIKVRVDMV	1.940	B*0801	CP	+
2A1-3					B*0801	CP	+
1A4-1	$UL28_{327–335}$	FRCPRRFCF	**FW**FRCPRRFCF	1.300	Cw*0702	DK	+
9G4-107	$UL16_{162–170}$	YPRPPGSGL	**SL**YPRPPGSGL	0.450	B*0702	DK	+
1A8-8	$UL105_{715–723}$	YADPFFLKY	**SL**YADPFFLKY	0.042	A*0101	CP	–